Factors Affecting the Oxidative Addition of Aryl Electrophiles to 1,1′-Bis(diphenylphosphino)ferrocenepalladium(η^2-methyl acrylate), an Isolable Pd[0] Alkene Complex

Anny Jutand,*[,†] King Kuok (Mimi) Hii,[‡,§] Mark Thornton-Pett,[⊥] and John M. Brown[‡]

Département de Chimie, Ecole Normale Supérieure, UMR CNRS 8640, 24 Rue Lhomond, 75231 Paris Cedex 05, France, Dyson Perrins Laboratory, South Parks Rd., Oxford OX1 3QY, U.K., and School of Chemistry, University of Leeds, Woodhouse Lane, Leeds LS2 9JT, U.K.

Received August 9, 1999

The title complex **3** has been synthesized and characterized by X-ray crystallography. It undergoes oxidative addition with aryl triflates and iodides by a nondissociative mechanism in THF. The Heck addition product methyl cinnamate was detected at traces from the reaction with phenyl triflate, and from iodobenzene the direct oxidative addition product was characterized. The addition of halides or acetate salts to the system led to modest effects on the rate of oxidative addition of aryl triflates, but resulted in neutral arylpalladium(II) complexes. Addition of lithium or europium salts enhanced the reaction rate, the effect being most pronounced with $Eu(OTf)_3$, possibly through promotion of a competing dissociative pathway.

Introduction

The mechanism of the Heck reaction continues to excite interest and some controversy.[1] In previous work the nature of the reactive intermediates has been considered by electrochemical techniques,[2] by NMR, or by mass spectrometry.[3] In the course of this some attention has been given to the reactivity of aryl triflates toward zerovalent palladium complexes.[4] In NMR studies that simulate the catalytic cycle but under stoichiometric conditions, breakdown of the Heck addition product **1** in the presence of proton sponge and excess alkene **2** leads to the alkenepalladium complex 1,1′-bis(diphenylphosphino)ferrocenepalladium(η^2-methyl acrylate), (dppf)Pd(MeA), **3** (Scheme 1).[5] This can be separately synthesized from the corresponding $PdCl_2$ complex **4** and is moderately stable. Here we report an electrochemical study of complex **3** toward the oxidative addition of aryl electrophiles, both triflates and iodides. This enables us to present a comparison between the behavior of a stable Pd[0] alkene complex and other potential catalyst precursors, such as $Pd(PPh_3)_4$,[4] as well as those generated in situ from phosphines and $Pd(dba)_2$ (dba = dibenzylidene acetone), reported in earlier work.[6] Previous experiments with $Pd(PPh_3)_4$ had revealed that chloride anions have an accelerating effect on the rate of the oxidative addition of aryl triflates, as

Scheme 1. Synthetic Route to Complex 3 and Its Role in the Breakdown of an Observed Intermediate in Heck Chemistry

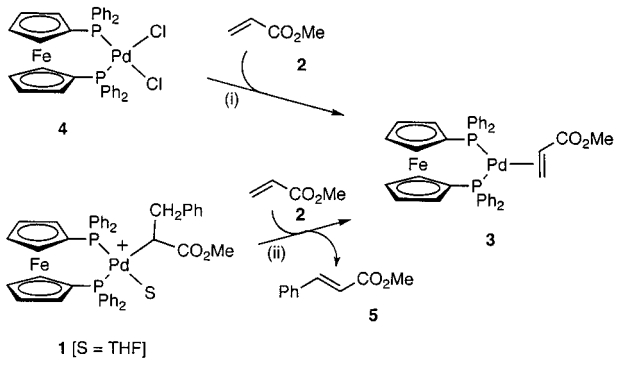

(i) Li_2COT, THF, -78 °C - 0 °C, xs. **2** or $NaBH_4$, THF/EtOH, xs. **2**

(ii) $C_{10}H_6(NMe_2)_2$, -40 °C, **2**.

† Département de Chimie, Ecole Normale Supérieure.
‡ Dyson Perrins Laboratory.
§ Currently at Department of Chemistry, King's College London, Strand, London WC2R2LS, U.K.
⊥ University of Leeds.

(1) For possible intervention of palladium(IV) intermediates in specific circumstances see: (a) Ohff, M.; Ohff, A.; Van der Boom, M. E.; Milstein, D. *J. Am. Chem. Soc.* **1997**, *119*, 11687. (b) Shaw, B. L. *New J. Chem.* **1998**, *22*, 77. (c) Shaw, B. L.; Perera, S. D.; Staley, E. A. *Chem. Commun.* **1998**, 1361.

(2) (a) Amatore, C.; Jutand, A.; M'Barki, M. A. *Organometallics* **1992**, *11*, 3009. (b) Amatore, C.; Carré, E.; Jutand, A.; M'Barki, M. A. *Organometallics* **1995**, *14*, 1818. (c) Amatore, C.; Carré, E., Jutand, A.; M'Barki, M. A.; Meyer, G. *Organometallics* **1995**, *14*, 5602.

(3) (a) Brown, J. M.; Guiry, P. J. *Inorg. Chim. Acta* **1994**, *220*, 249. (b) Brown, J. M.; Perez-Torrente, J. J.; Alcock, N. W.; Clase, H. J. *Organometallics* **1995**, *14*, 207. (c) Brown, J. M.; Hii, K. K. *Angew. Chem., Int. Ed. Engl.* **1996**, *35*, 657. (d) Hii, K. K.; Claridge, T.; Brown, J. M. *Angew. Chem., Int. Ed. Engl.* **1997**, *36*, 984.

(4) Jutand, A.; Mosleh, A. *Organometallics* **1995**, *14*, 1810.

(5) Hii, K. K.; Brown J. M. Manuscript in preparation.

(6) (a) Amatore, C.; Jutand, A.; Khalil, F.; M'Barki, M. A.; Mottier, L. *Organometallics* **1993**, *12*, 3168. (b) Amatore, C.; Broeker, G.; Jutand, A.; Khalil, F. *J. Am. Chem. Soc.* **1997**, *119*, 5176. (c) Amatore, C.; Jutand, A.; Meyer, G. *Inorg. Chim. Acta* **1998**, *273*, 76. (d) Amatore, C.; Jutand, A.; Meyer, G.; Atmani, H.; Khalil, F.; Chahdi, F. O. *Organometallics* **1998**, *17*, 2958.

10.1021/om9906417 CCC: $18.00
Publication on Web 11/17/1999

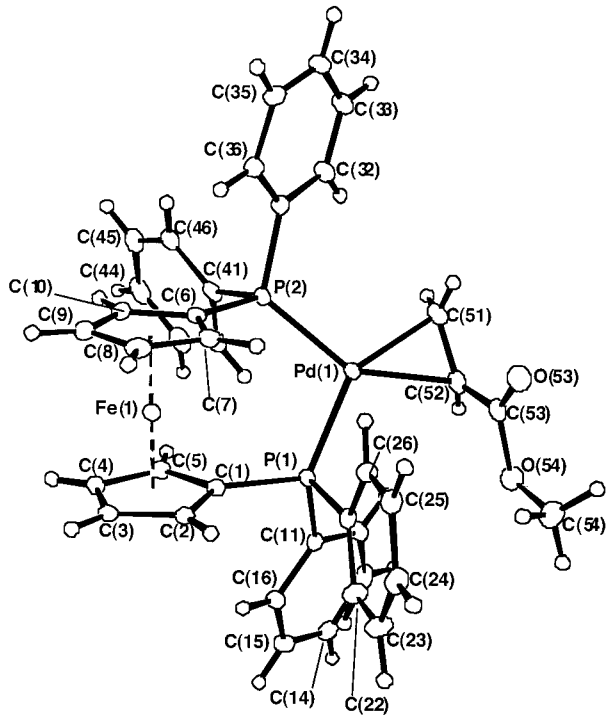

Figure 1. X-ray structure of complex **3**, with numbering corresponding to the assignments in Tables 1 and 2.

well as on the structure of the complex formed in this reaction.[4] Due to current interest in the role of potential promoters[7] for catalytic Heck reactions, we initiated a study of the effect of polar addends on the oxidative addition of complex **3** with aryl triflates.

Results and Discussion

Synthesis and Characterization of Complex 3. In situ reduction of diphosphinepalladium dihalides with cyclooctatetraene dianion gives an η^2-COT complex which may be used as a precursor to other alkene complexes.[8] It is possible to prepare the complex (dppf)-Pd(MeA), **3**, in this way, and it proved to be reasonably stable in the solid state. In solution the ^{31}P NMR is a closely spaced AB quartet (17.3, 21.4 ppm, $J_{PP} = 5$ Hz), reasonably sharp at ambient temperature. Rapid intermolecular exchange ($k_{exchange}$ = ca. 10^3 M^{-1} s^{-1} at 20 °C) was demonstrated by severe line broadening of ^{31}P resonances observed on sequential addition of methyl acrylate to the solution. The isolated complex does not show a sufficiently stable parent ion to allow satisfactory MS characterization by FAB or electrospray methods.

Crystallization of a sample from toluene/hexane in the presence of excess methyl acrylate gave pale orange plates. The X-ray structure is represented in Figure 1, and selected bond lengths and angles are shown in Tables 1 and 2. The palladium complex is monomeric with a square planar geometry around palladium and with the alkene η^2-coordinated to the metal in the P−Pd−P plane. In general the bond lengths and distances are unexceptional.[9]

Table 1. Interatomic Distances (Å) with esd's in Parentheses

Fe(1)−C(6)	2.040(2)	Fe(1)−C(7)	2.042(2)
Fe(1)−C(5)	2.042(2)	Fe(1)−C(1)	2.048(2)
Fe(1)−C(10)	2.056(2)	Fe(1)−C(2)	2.059(2)
Fe(1)−C(3)	2.064(2)	Fe(1)−C(4)	2.065(2)
Fe(1)−C(8)	2.066(2)	Fe(1)−C(9)	2.069(2)
C(1)−C(2)	1.437(3)	C(1)−C(5)	1.437(3)
C(1)−P(1)	1.821(2)	C(2)−C(3)	1.425(3)
C(3)−C(4)	1.424(3)	C(4)−C(5)	1.426(3)
C(6)−C(10)	1.431(3)	C(6)−C(7)	1.445(3)
C(6)−P(2)	1.808(2)	C(7)−C(8)	1.424(3)
C(8)−C(9)	1.420(3)	C(9)−C(10)	1.417(3)
P(1)−C(21)	1.831(2)	P(1)−C(11)	1.831(2)
C(11)−C(12)	1.395(3)	C(11)−C(16)	1.403(3)
C(12)−C(13)	1.393(3)	C(13)−C(14)	1.386(3)
C(14)−C(15)	1.388(3)	C(15)−C(16)	1.389(3)
C(21)−C(26)	1.395(3)	C(21)−C(22)	1.401(3)
C(22)−C(23)	1.391(3)	C(23)−C(24)	1.389(3)
C(24)−C(25)	1.383(3)	C(25)−C(26)	1.391(3)
P(2)−C(41)	1.839(2)	P(2)−C(31)	1.839(2)
C(31)−C(36)	1.398(3)	C(31)−C(32)	1.400(3)
C(32)−C(33)	1.389(3)	C(33)−C(34)	1.396(3)
C(34)−C(35)	1.387(3)	C(35)−C(36)	1.394(3)
C(41)−C(46)	1.394(3)	C(41)−C(42)	1.394(3)
C(42)−C(43)	1.395(3)	C(43)−C(44)	1.390(4)
C(44)−C(45)	1.389(4)	C(45)−C(46)	1.393(3)
Pd(1)−P(1)	2.3234(5)	Pd(1)−P(2)	2.3089(5)
Pd(1)−C(51)	2.122(2)	Pd(1)−C(52)	2.160(2)
C(51)−C(52)	1.414(3)	C(51)−H(51a)	1.00(3)
C(51)−H(51b)	0.96(3)	C(52)−C(53)	1.467(3)
C(52)−H(52)	0.92(3)	C(53)−O(53)	1.212(3)
C(53)−O(54)	1.362(3)	O(54)−C(54)	1.443(3)

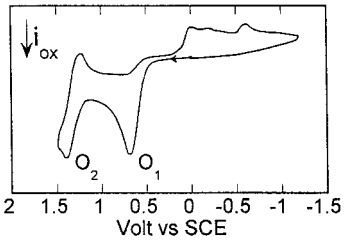

Figure 2. Cyclic voltammetry of (dppf)Pd(MeA), **3** (2 mmol dm^{-3}), in THF (containing *n*-Bu_4NBF_4, 0.3 mol dm^{-3}) at a steady gold disk electrode (i.d. = 2 mm) with a scan rate of 0.2 V s^{-1}, at 20 °C.

Arylpalladium(II) Complexes Formed in the Oxidative Addition of Aryl Triflates to Complex 3. Cyclic voltammetry performed on a solution of complex **3** (2 mmol dm^{-3}) in THF (containing *n*-Bu_4NBF_4, 0.3 mol dm^{-3}) exhibited two successive oxidation peaks at $E^p_{O1} = +0.73$ V (bielectronic, irreversible) and $E^p_{O2} = +1.41$ V vs SCE (monoelectronic, reversible) (Figure 2).

Addition of iodobenzene resulted in gradual conversion into a new complex (eq 1), which displayed two new oxidation peaks at +0.94 V (irreversible) and +1.16 V (reversible). This species and its ^{31}P NMR spectrum (Table 3) were found to be identical to those of an

(7) For anionic addends influencing Heck reactions see: (a) Cabri, W.; Candiani, I. *Acc. Chem. Res.* **1995**, *28*, 2, and references therein. (b) Overman, L. E.; Poon, D. J. *Angew. Chem., Int. Ed. Engl.* **1997**, *36*, 518.

(8) (a) Brown, J. M.; Cooley, N. A. *Organometallics* **1990**, *9*, 353. (b) Schager, F.; Haack, K. J.; Mynott, R.; Rufinska, A.; Porschke, K. R. *Organometallics* **1998**, *17*, 807.

(9) For some prior examples of 16-electron Pd alkene complexes see: (a) Hodgson, M.; Parker, D.; Taylor, R. J.; Ferguson, G. *J. Chem. Soc., Chem. Commun.* **1987**, 1309. (b) Benn, R.; Betz, P.; Goddard, R.; Jolly, P. W.; Kokel, N.; Kruger, C.; Topalovic, I. *Z. Naturforsch. B* **1991**, *46*, 1395. (c) Herrmann, W. A.; Thiel, W. R.; Brossmer, C.; Öfele, K.; Priermeier, T.; Scherer, W. *J. Organomet. Chem.* **1993**, *461*, 51. (d) Fawcett, J.; Kemmitt, R.; Russell, D. R.; Serindag, O. *J. Organomet. Chem.* **1995**, *486*, 171. (e) Goddard, R.; Hopp, G.; Jolly, P. W.; Kruger, C.; Mynott, R.; Wirtz, C. *J. Organomet. Chem.* **1995**, *486*, 163.

Table 2. Angles between Interatomic Vectors (deg) with esd's in Parentheses

C(6)−Fe(1)−C(7)	41.47(8)	C(6)−Fe(1)−C(5)	111.72(8)
C(7)−Fe(1)−C(5)	140.78(8)	C(6)−Fe(1)−C(1)	110.23(8)
C(7)−Fe(1)−C(1)	111.37(8)	C(5)−Fe(1)−C(1)	41.15(7)
C(6)−Fe(1)−C(10)	40.89(8)	C(7)−Fe(1)−C(10)	68.64(8)
C(5)−Fe(1)−C(10)	111.54(8)	C(1)−Fe(1)−C(10)	138.45(8)
C(6)−Fe(1)−C(2)	137.90(8)	C(7)−Fe(1)−C(2)	110.41(8)
C(5)−Fe(1)−C(2)	68.67(8)	C(1)−Fe(1)−C(2)	40.97(7)
C(10)−Fe(1)−C(2)	178.79(8)	C(6)−Fe(1)−C(3)	178.28(8)
C(7)−Fe(1)−C(3)	137.43(8)	C(5)−Fe(1)−C(3)	68.39(8)
C(1)−Fe(1)−C(3)	68.65(8)	C(10)−Fe(1)−C(3)	140.79(8)
C(2)−Fe(1)−C(3)	40.42(8)	C(6)−Fe(1)−C(4)	140.76(8)
C(7)−Fe(1)−C(4)	177.74(8)	C(5)−Fe(1)−C(4)	40.64(8)
C(1)−Fe(1)−C(4)	68.69(8)	C(10)−Fe(1)−C(4)	112.91(8)
C(2)−Fe(1)−C(4)	68.07(8)	C(3)−Fe(1)−C(4)	40.35(8)
C(6)−Fe(1)−C(8)	68.86(8)	C(7)−Fe(1)−C(8)	40.55(8)
C(5)−Fe(1)−C(8)	178.47(8)	C(1)−Fe(1)−C(8)	140.19(8)
C(10)−Fe(1)−C(8)	67.89(8)	C(2)−Fe(1)−C(8)	111.93(8)
C(3)−Fe(1)−C(8)	111.08(8)	C(4)−Fe(1)−C(8)	138.06(8)
C(6)−Fe(1)−C(9)	68.48(8)	C(7)−Fe(1)−C(9)	68.09(8)
C(5)−Fe(1)−C(9)	138.53(8)	C(1)−Fe(1)−C(9)	178.59(8)
C(10)−Fe(1)−C(9)	40.19(8)	C(2)−Fe(1)−C(9)	140.38(8)
C(3)−Fe(1)−C(9)	112.66(8)	C(4)−Fe(1)−C(9)	111.90(8)
C(8)−Fe(1)−C(9)	40.16(9)	C(2)−C(1)−P(1)	126.43(14)
C(2)−C(1)−C(5)	107.2(2)	C(2)−C(1)−Fe(1)	69.94(11)
C(5)−C(1)−P(1)	126.4(2)	P(1)−C(1)−Fe(1)	125.54(10)
C(5)−C(1)−Fe(1)	69.22(11)	C(3)−C(2)−Fe(1)	69.98(11)
C(3)−C(2)−C(1)	108.2(2)	C(4)−C(3)−C(2)	108.2(2)
C(1)−C(2)−Fe(1)	69.09(11)	C(2)−C(3)−Fe(1)	69.59(11)
C(4)−C(3)−Fe(1)	69.83(11)	C(3)−C(4)−Fe(1)	69.82(11)
C(3)−C(4)−C(5)	108.1(2)	C(4)−C(5)−C(1)	108.2(2)
C(5)−C(4)−Fe(1)	68.84(11)	C(1)−C(5)−Fe(1)	69.63(11)
C(4)−C(5)−Fe(1)	70.52(11)	C(10)−C(6)−P(2)1	28.0(2)
C(10)−C(6)−C(7)	106.9(2)	C(10)−C(6)−Fe(1)	70.16(11)
C(7)−C(6)−P(2)	125.1(2)	P(2)−C(6)−Fe(1)	126.51(10)
C(7)−C(6)−Fe(1)	69.35(11)	C(8)−C(7)−Fe(1)	70.63(11)
C(8)−C(7)−C(6)	108.0(2)	C(9)−C(8)−C(7)	108.1(2)
C(6)−C(7)−Fe(1)	69.18(11)	C(7)−C(8)−Fe(1)	68.81(11)
C(9)−C(8)−Fe(1)	70.04(12)	C(10)−C(9)−Fe(1)	69.39(11)
C(10)−C(9)−C(8)	108.5(2)	C(9)−C(10)−C(6)	108.5(2)
C(8)−C(9)−Fe(1)	69.80(12)	C(6)−C(10)−Fe(1)	68.95(1
C(9)−C(10)−Fe(1)	70.42(12)	C(1)−P(1)−C(11)	100.04(9)
C(1)−P(1)−C(21)	99.01(9)	C(1)−P(1)−Pd(1)	120.80(7)
C(21)−P(1)−C(11)	104.13(9)	C(11)−P(1)−Pd(1)	117.75(7)
C(21)−P(1)−Pd(1)	112.28(7)	C(12)−C(11)−P(1)	119.4(2)
C(12)−C(11)−C(16)	118.7(2)	C(13)−C(12)−C(11)	120.7(2)
C(16)−C(11)−P(1)	122.0(2)	C(13)−C(14)−C(15)	120.0(2)
C(14)−C(13)−C(12)	120.0(2)	C(15)−C(16)−C(11)	120.5(2)
C(14)−C(15)−C(16)	120.1(2)	C(26)−C(21)−P(1)	116.9(2)
C(26)−C(21)−C(22)	118.8(2)	C(23)−C(22)−C(21)	120.2(2)
C(22)−C(21)−P(1)	124.0(2)	C(25)−C(24)−C(23)	119.8(2)
C(24)−C(23)−C(22)	120.3(2)	C(25)−C(26)−C(21)	120.7(2)
C(24)−C(25)−C(26)	120.1(2)	C(6)−P(2)−C(31)	100.82(9)
C(6)−P(2)−C(41)	101.69(9)	C(6)−P(2)−Pd(1)	116.41(7)
C(41)−P(2)−C(31)	102.61(9)	C(31)−P(2)−Pd(1)	118.73(7)
C(41)−P(2)−Pd(1)	114.11(7)	C(36)−C(31)−P(2)	122.4(2)
C(36)−C(31)−C(32)	118.9(2)	C(33)−C(32)−C(31)	120.6(2)
C(32)−C(31)−P(2)	118.6(2)	C(35)−C(34)−C(33)	119.6(2)
C(32)−C(33)−C(34)	120.1(2)	C(35)−C(36)−C(31)	120.3(2)
C(34)−C(35)−C(36)	120.4(2)	C(46)−C(41)−P(2)	122.2(2)
C(46)−C(41)−C(42)	119.0(2)	C(41)−C(42)−C(43)	120.5(2)
C(42)−C(41)−P(2)	118.7(2)	C(45)−C(44)−C(43)	119.8(2)
C(44)−C(43)−C(42)	120.0(2)	C(45)−C(46)−C(41)	120.6(2)
C(44)−C(45)−C(46)	120.1(2)	C(51)−Pd(1)−P(2)	107.37(7)
C(51)−Pd(1)−C(52)	38.55(9)	C(51)−Pd(1)−P(1)	147.94(7)
C(52)−Pd(1)−P(2)	145.93(6)	P(2)−Pd(1)−P(1)	104.48(2)
C(52)−Pd(1)−P(1)	109.51(6)	C(52)−C(51)−H(51a)	118(2)
C(52)−C(51)−Pd(1)	72.16(12)	C(52)−C(51)−H(51b)	119(2)
Pd(1)−C(51)−H(51a	110(2)	H(51a)−C(51)−H(51b)	118(2)
Pd(1)−C(51)−H(51b	108(2)	C(51)−C(52)−Pd(1)	69.28(12)
C(51)−C(52)−C(53)	121.0(2)	C(51)−C(52)−H(52)	123(2)
C(53)−C(52)−Pd(1)	108.39(14)	Pd(1)−C(52)−H(52)	108(2)
C(53)−C(52)−H(52)	114(2)	O(53)−C(53)−C(52)	126.5(2)
O(53)−C(53)−O(54)	121.9(2)	C(53)−O(54)−C(54)	114.8(2)
O(54)−C(53)−C(52)	111.7(2)		

authentic sample of the known neutral complex PhPdI(dppf).[3a]

$$(\text{dppf})\text{Pd(MeA)} + \text{ArI} \rightarrow \text{ArPdI(dppf)} + \text{MeA} \quad (1)$$

In contrast, addition of aryl triflates such as 4-NO_2−C_6H_4−OTf, 3,5-CF_3−C_6H_3−OTf, or PhOTf to complex **3** resulted in an electrolyte that did not show any identifiable ^{31}P NMR signals, even though it displayed a new reversible oxidation peak at +1.3 V in each case. This was ascribed to the instability of the resulting cationic arylpalladium triflate complex (eq 2), which decomposes at room temperature.[3c]

$$(\text{dppf})\text{Pd(MeA)} + \text{ArOTf} \rightarrow \text{ArPd(dppf)}^+ + \text{TfO}^- + \text{MeA} \quad (2)$$

A parallel ^{1}H NMR experiment[10] carried out in THF-d_8 with PhOTf using similar concentrations showed the disappearance of the complex **3** over 18 h, with concurrent release of methyl acrylate **2**. Due however to the relatively low concentration of the methyl acrylate, only 2% of methyl cinnamate **5**, the formal product of a Heck reaction, was observed.

The oxidative addition of aryl triflates to complex **3** performed in the presence of anions (Cl^-, I^-, or AcO^-) led to clean formation of neutral arylpalladium(II) complexes (eq 3). These were found to have oxidation peaks and ^{31}P NMR signals identical to independently prepared ArPdCl(dppf), ArPdI(dppf), and ArPd(OAc)(dppf) complexes[11] (Tables 3, 4). Analogous neutral complexes had also been obtained in the related reaction with $Pd(PPh_3)_4$.[4]

$$\{(\text{dppf})\text{Pd(MeA)} + \text{X}^-\} + \text{ArOTf} \rightarrow \text{ArPdX(dppf)} + \text{MeA} + \text{TfO}^- \quad (3)$$
$$\text{X} = \text{Cl}^-, \text{I}^-, \text{AcO}^-$$

On the other hand, the nature of the cationic component of the added salt (Li^+, Eu^{3+}) had no effect on the structure of the complex formed in the oxidative addition of aryl triflates.

The Rate and Mechanism of the Oxidative Addition of Aryl Electrophiles to Complex 3. The kinetics of the oxidative addition of complex **3** to aryl triflates and iodides was monitored by electrochemical techniques by recording the decay of its first oxidation peak O_1 (the current being proportional to the concentration of the palladium(0) complex). Previous work[4,6] has shown that amperometry is the most convenient technique to monitor the kinetics of oxidative additions of palladium(0) complexes. This involves polarization of a rotating disk electrode at +0.6 V (first oxidation wave O_1) in a solution of complex **3**. The decay of the oxidation current of (dppf)Pd(MeA) was subsequently recorded as a function of time in the presence of an excess of the aryl triflate (Figure 3a). The oxidation current of complex **3** dropped to zero, indicating that the products formed in the oxidative addition were not electroactive at +0.6 V (see Table 3). A plot of $\ln([Pd^0]/[Pd^0]_0)$ versus time resulted in a straight line (Figure 3b).

(10) We thank Dr. T. D. W. Claridge for help with this experiment. A 2 mM solution of complex **3** in THF-d_8 containing 0.3 M electrolyte and 50 equiv of phenyl triflate was examined by ^{1}H NMR spectroscopy at 500 MHz. The disappearance of the signals corresponding to complex **3** was monitored, and these were integrated against the emergence of new peaks corresponding to methyl cinnamate and methyl acrylate.

(11) ArPdI(dppf) was prepared according to procedures described in a previous reference.[3a] The corresponding acetate and chloride complexes were obtained by substitution of the anionic ligand at −60 °C, with AgOAc and $AgBF_4$/*n*-Bu_4NCl, respectively.

Table 3. Oxidation Peak Potential of the Arylpalladium(II) Complexes Formed in the Oxidative Addition of Pd(dppf)(MA) to Aryl Triflates and Iodides as a Function of the Addend

entry	ArX	addend (equiv/Pd)	E^{p}_{ox} (V vs SCE)[a]	E^{p}_{ox} (V vs SCE)[a]
1	4-NO_2−C_6H_4−OTf	none	+1.34	
2		3.4 *n*-Bu_4N**Cl**		+1.21, ArPd**Cl**(dppf)
3		3.4 *n*-Bu_4N**OAc**		+1.11, ArPd(**OAc**)(dppf)
4		$LiBF_4$	+1.33	
5		$Zn(BF_4)_2$	+1.33	
6		$Eu(tfc)_3$	+1.32	+1.14
7	3,5-CF_3−C_6H_3−OTf	none	+1.34	
8		3.4 *n*-Bu_4N**Cl**		+1.20, ArPd**Cl**(dppf)
9	Ph-OTf	none	nd	
10		3.4 *n*-Bu_4N**Cl**		+1.15, PhPd**Cl**(dppf)
11		3.4 *n*-Bu_4N**I**		+0.94, PhPd**I**(dppf)
12	PhI	none		+0.94, PhPd**I**(dppf)
13		3 $Eu(OTf)_3$		+0.82, +0.97

[a] Potentials at a steady gold electrode (i.d. 2 mm) with a scan rate of 0.2 V s^{-1} at 20 °C.

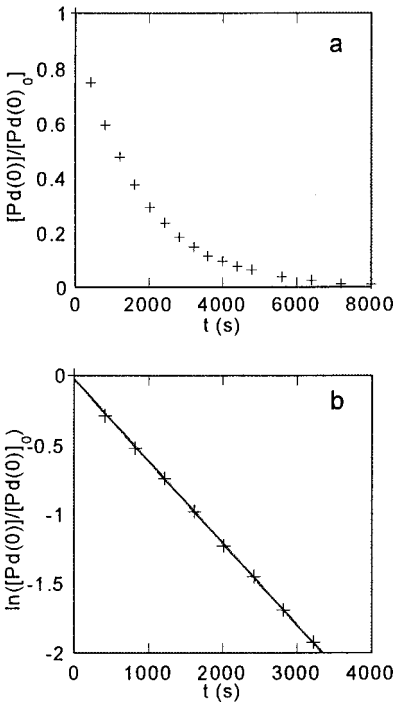

Figure 3. Oxidative addition of 4-NO_2−C_6H_4−OTf (100 mmol dm^{-3}) to (dppf)Pd(MeA), **3** (2 mmol dm^{-3}), in THF (containing *n*-Bu_4NBF_4, 0.3 mol dm^{-3}) at 40 °C. (a) Variation of $[Pd]/[Pd]_0$ as a function of time ($[Pd]/[Pd]_0 = i/i_0$: i, oxidation current of O_1 at time t; i_0, initial oxidation current of O_1). (b) Variation of $\ln([Pd]/[Pd]_0)$ as a function of time.

$$\ln([Pd^0]/[Pd^0]_0) = -k_{app}t \qquad (4)$$

$[Pd^0]/[Pd^0]_0 = i/i_0$, where i is the oxidation current of O_1 at time t and i_0 is the initial oxidation current of O_1.

The apparent rate constant k_{app} of the oxidative addition (eq 4) was given by the slope (Table 4). As was observed for palladium(0) complexes ligated by monodentate phosphines,[4] the oxidative addition of (dppf)-Pd(MeA) proceeds faster when the aryl triflate is substituted by electron-withdrawing groups; and aryl triflates are less reactive than the corresponding iodides (entries 10 and 13, Table 4).

For a similar (diphosphine)Pd(alkene) complex, generated in situ from a mixture of $Pd(dba)_2$ and 1 equiv of dppf, a dynamic exchange was found to exist between (dppf)Pd(dba) and a less ligated complex (eq 5).[6b] Although the 14-electron Pd(dppf) complex is more reactive than (dppf)Pd(dba), its lower concentration means that both complexes react with PhI in parallel, resulting in a reaction order that differs from one in PhI (i.e., $k_{app} = a + b[PhI]$).[6b]

$$(dppf)Pd(dba) \rightleftarrows Pd(dppf) + dba \qquad (5)$$

To investigate whether a similar equilibrium operates in our present system (eq 6 in Scheme 2) and to determine the effective reactive species, the kinetics of the oxidative addition was also probed with the more reactive iodobenzene.

A plot of $\ln([Pd^0]/[Pd^0]_0)$ as a function of time afforded a series of straight lines whose slopes (k_{app}) were found to vary linearly with the iodobenzene concentration with a zero intercept (Figure 4a) ($\ln([Pd^0]/[Pd^0]_0) = -k_{app}t = -k[PhI]t$). This means that the reaction order in PhI is unity and implies that only one palladium(0) complex, either complex **3** or Pd(dppf), is reactive in the oxidative addition. Since the kinetic law, $\ln([Pd^0]/[Pd^0]_0) - [Pd^0]/[Pd^0]_0 + 1 = -k_{app}t$, was not obeyed, as would be expected if Pd(dppf) were the sole reactive species, this requires that complex **3** is the only reactive species in the oxidative addition (Scheme 2). Further proof was provided when no significant decelerating effect was observed when the reaction was carried out in the presence of added methyl acrylate.[12]

The surprising lack of participation of Pd(dppf) in our present system suggests that (i) its concentration in equilibrium 6 is considerably smaller than in equilibrium 5 and/or (ii) complex **3** is more reactive per se than (dppf)Pd(dba). The presence of one free dba for the in situ case prevented any more rigorous comparison of the two experiments.

The kinetic law, expressed as $\ln([Pd]/[Pd]_0) = -k[ArX]t$, allows the determination of the rate constant k of the oxidative addition of complex **3** to aryl triflates and iodides (Table 4). When compared to another well-investigated palladium(0) complexes, complex **3** is considerably less reactive toward iodobenzene than

(12) When cyclic voltammetry was performed at low scan rate (0.2 V s^{-1}) on a solution of (dppf)Pd(MeA) directly in reduction, the reduction peak of methyl acrylate at −2.2 V vs SCE was not detected. This means that equilibrium 6 has not shifted significantly to the right-hand side despite continuous reduction of MeA in the diffusion layer (CE mechanism[13]). The equilibrium is thus considerably in favor of (dppf)Pd(MeA), and the complex is not very labile, in accord with NMR observations (ref 10).

Table 4. Oxidative Addition of (dppf)Pd(MeA)[a] to Aryl Triflates and Iodides in THF: Role of Addends

entry	ArX	[ArX]/[Pd]	*T* (°C)	addend (equiv/Pd)	$10^4\ k_{app}$ (s^{-1})	10^3 k ($M^{-1}\ s^{-1}$)[b]	^{31}P NMR δ ppm [J_{PP} Hz]
1	4-NO_2−C_6H_4−OTf	50	40	none	5.9	5.9	*c*
2		50	40	*n*-Bu_4NCl (3.4)	4.6		ArPdCl(dppf) 11.7; 31.4 [30]
3		50	40	*n*-Bu_4NOAc (3.4)	6.4		ArPd(OAc)(dppf) 11.9; 31.5 [30]
4		50	40	$LiBF_4$ (1)	8.1		*c*
5		50	40	$LiBF_4$[d] (20)	9.2		*c*
6		50	40	$Eu(hfc)_3$ (3)	7.3		*c*
7		50	40	$Eu(OTf)_3$[d] (3)	46		*c*
8	3,5-CF_3−C_6H_3−OTf	50	25	none	1.2	1.2	*c*
9		50	25	*n*-Bu_4NCl (3)	0.8		ArPdCl(dppf) 12.3; 32.0 [29]
10	PhOTf	100	25	none	2.3	1.1	*c*
11		100	25	*n*-Bu_4NCl (3)	1.0		PhPdCl(dppf) 10.2; 31.3 [32]
12		100	25	*n*-Bu_4NI (3)	nd		PhPdI(dppf) 8.2; 26.4 [35]
13	PhI	50	25	none	5.8	5.8	PhPdI(dppf)
14		50	25	$Eu(OTf)_3$[d] (3)	53.8		*c*

[a] [(dppf)Pd(MeA)] = 2 mmol dm^{-3}. [b] For the definition of *k*, see Scheme 2. [c] No identifiable signals. [d] Premixed with ArX.

Scheme 2. Oxidative Addition of Aryl Electrophiles to Complex 3

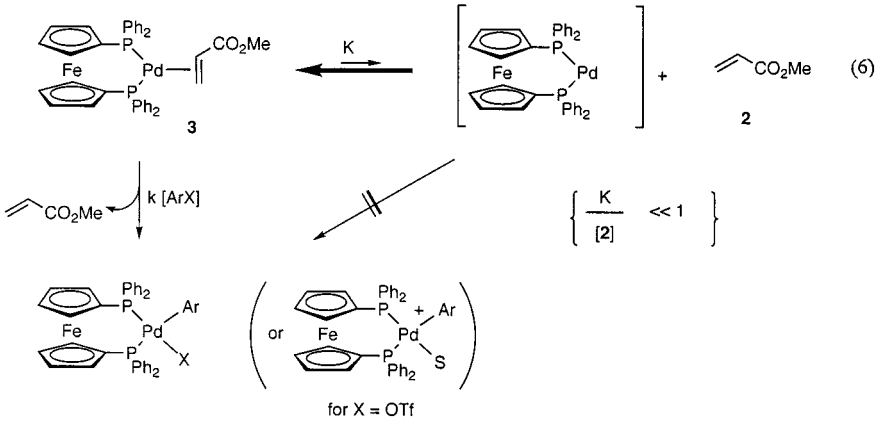

$Pd(PPh_3)_4$.[6a] The ratio of the two rate constants is approximately 1:4300, but the corresponding ratio for phenyl triflate is ca. 1:5.[4]

Addition of 3 equiv of Cl^- has a slight decelerating effect on the rate of the oxidative addition to aryl triflates (entries 1,2; 8,9; 10,11, Table 4). The close vicinity of the oxidation peaks of complex **3** and Cl^- hampers investigations at higher chloride concentrations. The opposite effect was observed for $Pd(PPh_3)_4$, where $Pd(PPh_3)_2Cl^-$ species are involved in promoting the rate of oxidative addition.[4,14] This implies that Cl^- binds less strongly to Pd(dppf) than to $Pd(PPh_3)_2$, even though trace amounts of the anionic species $Pd(dppf)Cl^-$ have been detected in a solution mixture of complex **3** and *n*-Bu_4NCl by electrospray mass spectrometry.[15]

Addition of $Eu(OTf)_3$ has a strong accelerating effect (ca. 10-fold) on the rate of the oxidative addition of both aryl triflates and aryl halides to complex **3** (entries 1,7 and 13,14 in Table 4, Figure 4b). The hexacoordinated, weaker Lewis acidic $Eu(hfc)_3$ was found to be less effective (entries 1, 6, 7 in Table 4). $LiBF_4$ had little effect, even when present at high concentration (entries 1, 4, 5 in Table 4). The observed acceleration by $Eu(OTf)_3$ in the oxidative addition probably arises from the complexation of the Lewis acid with ligated methyl acrylate. This promotes the dissociation of the alkene ligand from palladium(0), causing a shift in the equilibrium 6 (Scheme 2) to the more reactive 14-electron Pd(dppf) complex, thus enhancing the rate of the subsequent oxidative addition step. When 3 equiv of $Eu(OTf)_3$ was added to complex **3**, slow decomposition occurred, presumably via the same 14-electron complex Pd(dppf).[16]

(13) Bard, A. J.; Faulkner, L. R. *Electrochemical Methods*; Wiley: New York, 1980; pp 136−143.

(14) Amatore, C.; Azzabi, M.; Jutand, A. *J. Am. Chem. Soc.* **1991**, *113*, 8375.

(15) We thank Dr. R. T. Aplin for help with this experiment. A reaction mixture generated from complex **3** and 4.5 equiv of *n*-Bu_4NCl in methanol was introduced directly into the electrospray mass spectrometer operating in negative ion mode at room temperature, with methanol as the carrier solvent and a cone voltage of 30 V. A species corresponding to the ion $(dppf)PdCl^-$ was observed at *m*/*z* 695, 697 (^{106}Pd). No clear-cut evidence was obtained for the existence of any related P_2PdX anion (P_2 = dppf) under comparable conditions.

(16) The rate of decomposition was less than that of the oxidative addition; nevertheless the cation and the aryl derivative were added to the (dppf)Pd(MeA) solution as a premixed solution.

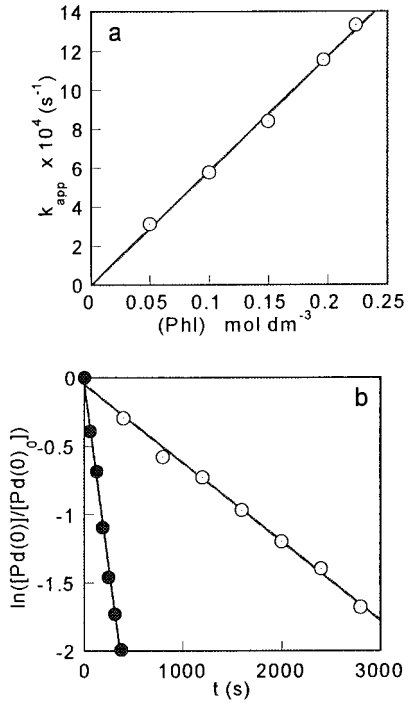

Figure 4. (a) Oxidative addition of iodobenzene to (dppf)-Pd(MeA), **3** (2 mmol dm^{-3}), in THF (containing *n*-Bu_4NBF_4, 0.3 mol dm^{-3}) at 25 °C. Variation of the apparent rate constant of the oxidative addition, k_{app} (s^{-1}), as a function of the iodobenzene concentration. Slope: $k = (5.8 \pm 0.1) \times 10^{-3}$ M^{-1} s^{-1}; $r = 0.998$. (b) Oxidative addition of (dppf)-Pd(MeA), **3** (2 mmol dm^{-3}), at 25 °C to (○) PhI (0.1 mol dm^{-3}) in the absence of $Eu(OTf)_3$; (●) PhI (0.1 mol dm^{-3}) and $Eu(OTf)_3$ (6 mmol dm^{-3}).

In summary, we have observed that the addition of anions generally does not have a significant effect on the rate of the oxidative addition of aryl triflates to complex **3**, but the nature of the resulting arylpalladium(II) complex was modified. In contrast, addition of certain cations operating as Lewis acids enhances the rate of oxidative addition of aryl triflates to complex **3** without altering the cationic nature of the complex formed by the reaction.

Related Catalytic Turnover Experiments. Experiments were first carried out on the coupling reaction between methyl acrylate and 4-nitrophenyl triflate, using complex **3** as precatalyst. The results are summarized in Table 5.

In the absence of addends, the reaction was fairly sluggish with an unfavorable product distribution, nitrobenzene **7** being formed as a side product (entry 1). The addition of lanthanide triflates (entries 2−6) increases the turnover rate with a worsening in the product distribution. Chloride salts (entries 7−11) improve selectivities dramatically, but with a corresponding reduction in turnover rates. Europium, copper, and hafnium chlorides (entries 9, 10, and 11) perform better than the alkali metal chlorides with respect to the rate of product formation. Fluoride salts were also used as addends, but again the product distribution was biased toward the reduction product, with no apparent enhancement in the reaction rate. Competition between reduction and coupling of aryl triflates has previously been observed by Cabri and co-workers, the reduction being attributed to hydride transfer from the α-carbon of NEt_3 to the Pd aryl cation and reductive elimination.[17]

Table 5. Results of Coupling between Methyl Acrylate and 4-Nitrophenyl Triflate 5, Using Complex 3 as Catalyst[a]

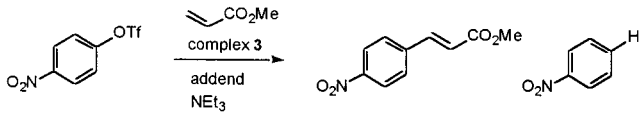

5 6 7

entry	added species	time/h	% conversion ArOTf	**6**:**7**
1	none	40	100	32:68
2	$Sc(OTf)_3$	17	94	0:100
3	$Yb(OTf)_3$	17	100	24:76
4	$Cu(OTf)_3$	64	34	16:84
5	$Sm(OTf)_3$	20	100	14:86
6	$Eu(OTf)_3$	40	100	37:63
7	$CeCl_3$	71	16	100:0
8	LiCl	64	45	100:0
9	$EuCl_3$	71	94	90:10
10	$CuCl_2$	94	100	100:0
11	$HfOCl_2$	71	100	100:0
12	LiF	120	97	20:80
13	CsF	41	96	34:66
14	SnF_4	120	91	54:46

[a] All experiments were carried out in THF at 65 °C, using 3 equiv of triethylamine as base and 5 mol % of addend where applicable. The conversion of 4-nitrophenyl triflate and product distribution were monitored by GC.

Summary and Conclusions

In this work we have isolated and characterized a stable palladium(0) P_2Pd[alkene] complex, (dppf)Pd-(MeA), **3**. We have demonstrated an exclusive partitioning of this P_2Pd[alkene] complex along the 16-electron oxidative addition pathway with aryl derivatives, without alkene dissociation. This is significantly different from a similar set of experiments reported for (dppf)-Pd(dba). Many of the recent studies involving Heck reactions with high turnover employ methyl acrylate and aryl halides, and it is important to recognize that, just as in the case of dba, the alkene reactant (and product) are electrophilic alkenes whose strong association to Pd(0) may diminish the turnover rate by enforcing a kinetically unfavorable mechanism of oxidative addition.

A further point of interest lies in the relative reactivities of Ph−I and Ph−OTf, differing here by a factor of 5. In the related addition of the same electrophiles to $Pd(PPh_3)_4$, around 10^4 greater discrimination is observed in favor of Ph−I. This is reminiscent of the wide variation in halide/tosylate rate ratios observed in aliphatic solvolysis.[18a,b] There could also be a change in the actual mechanism of the oxidative addition step as a function of the leaving group and/or ligand. If the comparable reactivity of the 16-electron Pd intermediate (dppf)Pd(MeA) with PhI and PhOTf is the consequence of a SNAr mechanism,[18c] then the greater difference in reactivity for PhI and PhOTf observed with the 14-

(17) Cabri, W.; Candiani, I.; Debernardinis, S.; Francalanci, F.; Penco, S.; Santi, R. *J. Org. Chem.* **1991**, *56*, 5796.

(18) (a) Kevill, D. N.; Abduljaber, M. H. *J. Chem. Soc., Perkin Trans. 2* **1995**, 1985. (b) Liu, K. T.; Tang, C. S. *J. Org. Chem.* **1996**, *61*, 1523, and references therein. (c) Fitton, P.; Rick, E. A. *J. Organomet. Chem.* **1971**, *28*, 287.

electron $Pd(PPh_3)_2$ implies more developed Pd−I bonding at the TS in that case.

The accelerating effect of $Eu(OTf)_3$ on the oxidative addition rate of either PhI or PhOTf to (dppf)Pd(MeA) is explicable if the carbonyl oxygen of coordinated acrylate is the site of Eu association. This would both increase the electrophilic character of the alkene and facilitate its dissociation, providing a significant concentration of the 14-electron (dppf)Pd[0] species, which then becomes the main channel for the oxidative addition.

The importance of anionic addends X^- (X = Cl, I, AcO) in the oxidative addition of aryl triflates is reiterated. Although there is no significant effect on the rate of the oxidative addition, the formation of neutral ArPdX(dppf) complexes may have important implications in the subsequent alkene insertion of Heck reactions.[2c,3b,7b]

Experimental Section

^{31}P NMR spectra were recorded on Bruker spectrometers (101 and 202 MHz) using H_3PO_4 as an external reference. ^1H NMR spectra were recorded on a Bruker spectrometer (500 MHz) and referenced to TMS.

Reagents. All experiments were performed under argon. THF (Acros) was distilled from sodium−benzophenone. The solvent was transferred to the cells according to standard Schlenk procedures. The dppf and methyl acrylate ligands were obtained commercially (Aldrich) and used without further purification. Iodobenzene (Acros) was filtered on neutral alumina and stored under argon. (dppf)$PdCl_2$,[19] Li_2(COT),[20] and aryl triflates[21] were prepared according to literature methods.

Synthesis of [(dppf)Pd(MeA)], 3. Li_2(COT) (0.26 M in diethyl ether, 2.7 mL, 0.7 mmol.) was added to a stirred suspension of (dppf)$PdCl_2$ (0.5 g, 0.7 mmol) in dry THF (20 mL) at −78 °C. The resulting deep red solution was treated with methyl acrylate (4 mL), and the reaction mixture was slowly warmed to room temperature, whereupon the solvent was removed under reduced pressure. Methanol was added to the residue, giving the required compound as a yellow solid. Yield: 0.39 g, 77%. IR (KBr disc): ν(C≡O) 1692 s cm^{-1}. ^{31}P (202 MHz, CD_2Cl_2): δ 17.3 (d, J_{PP} = 5 Hz), 21.4 (d, J_{PP} 5 Hz). ^1H (500 MHz): δ 7.8−7.3 (m, 20H, P*Ph*) 4.45 (m, 2H, *Cp*); 4.36 (m, 2H, *Cp*); 4.26 (m, 2H, *Cp*); 4.01 (m, 2H, *Cp*); 3.85 (ddd 1H, J_{PH} 8.0 Hz, J_{HH} 8.0, 11.0 Hz, H_a); 3.11 (s, 3H, CO_2Me); 3.00 (dd 1H, J_{PH} 8.0 Hz, J_{HH} 8.0 Hz, H_b); 2.82 (dd, 1H, J_{PH} 7.0 Hz, J_{HH} 11.0 Hz, H_c).

The alkene complex was successfully prepared in related experiments where the Li_2(COT) was replaced by $NaBH_4$ in THF/EtOH at −60 °C.

Electrochemical Setup and Procedure for Cyclic Voltammetry and Amperometry. Cyclic voltammetry was performed with a homemade potentiostat and a waveform generator, Tacussel (GSTP4). The voltammograms were recorded on a Nicolet 3091 digital oscilloscope. Experiments were carried out in a thermostated three-electrode cell connected to a Schlenk line, under argon. The counter electrode was a platinum wire of ca. 1 cm^2 apparent surface area; the reference was a saturated calomel electrode (Tacussel) separated from the solution by a bridge (3 mL) filled with a 0.3 M *n*-Bu_4NBF_4 solution in THF. A 20 mL sample of THF containing 0.3 M *n*-Bu_4NBF_4 was poured into the cell. A 30 mg (2 mmol dm^{-3}) sample of (dppf)Pd(MeA) was then added. The cyclic voltammetry was performed at a steady gold disk electrode (i.d. = 2 mm) with a scan rate of 0.2 V s^{-1}.

The kinetic measurements were performed by amperometry at a rotating gold disk electrode (i.d. = 2 mm, Tacussel EDI 65109) with an angular velocity of 105 rad s^{-1} (Tacussel controvit). The RDE was polarized at +0.6 V on the first oxidation wave O_1 of (dppf)Pd(MeA). After addition of the required amount of the aryl triflate or iodide, the oxidation current was recorded as a function of time up to 100% conversion. In another set of experiments, the desired amount of addend was introduced before the addition of the aryl derivatives (in the case of added anions) or together with the aryl derivatives (in the case of added cations).

Table 6. Crystallographic Data for Complex 3

empirical formula	$C_{38}H_{34}FeO_2P_2Pd$
M	746.84
size (mm)	0.26 × 0.10 × 0.07
temp (K)	180
cryst syst	monoclinic
space group	$P2_1/c$
unit cell dimens	
a (Å)	15.3313(1)
b (Å)	10.7804(1)
c (Å)	19.4659(2)
β (deg)	102.0370(6)
V (Å^3)	3146.54(5)
Z	4
ρ_{calc} (Mg m^{-3})	1.577
μ (mm^{-1})	1.169
max, min transmn	0.923, 0.751
F(000)	1520
θ range (deg)	1.36−26.0
no. reflns collected	77911
no. indep reflns	6179
no. reflns with $F_o^2 > 2\sigma(F_o^2)$	5643
R_{int}	0.0132
no. of params	411
goodness of fit on F^2	1.035
R_1 ($F^2 > 2\sigma F^2$)	0.0254
wR (all data, F^2)	0.0674
largest peak, hole (e Å^{-3})	0.422, −0.826

X-ray structural analysis of 3. Single yellow prismatic crystals were obtained by diffusion of *n*-hexane into a CH_2Cl_2 solution at room temperature. Crystal data and details of data collection and refinement are summarized in Table 6. All crystallographic measurements were carried out at 180 K on a Nonius Kappa CCD area-detector diffractometer using Mo Kα radiation (λ = 0.71073 Å). The detector was positioned 25 mm from the crystal, and data were collected as follows: "head-on" data (χ = 0°) as 360 oscillation frames of 60 s exposure time with 1° rotation in ϕ; "cusp" data (χ = 90°) as 35 frames of 60 s exposure time and 1° ω rotations, collected at each of four different ϕ settings. The package DENZO-SMN[22] was used for indexing, unit cell refinement, and data integration and scaling. The data were corrected for Lorentz and polarization effects using Scalepack.[23] Subsequently an empirical absorption correction based on redundant and symmetry-equivalent data was applied using the program SORTAV.[24] The structure was solved by direct methods (SHELXS-97)[25] and was developed by alternating cycles of least-squares refinement (on F^2) and Fourier difference syntheses (SHELXL-97).[25] All non-hydrogen atoms were refined with anisotropic displacement parameters. All hydrogen atoms were constrained to idealized positions (using a riding model with free rotation for methyl groups and fixed isotropic displacement parameters).

(19) Hayashi, T.; Konishi, M.; Kobori, Y.; Kumada, M.; Higuchi, T.; Hirotsu. K. *J. Am. Chem. Soc.* **1984**, *106*, 158.
(20) Katz, T.; Garratt, P. J. *J. Am. Chem. Soc.* **1964**, *86*, 4876.
(21) Hirota, K.; Isobe, Y.; Maki, Y. *J. Chem. Soc., Perkin Trans. 1* **1989**, 2513.
(22) Otwinowski, Z.; Minor, W. *Methods Enzymol.* **1996**, *276*, 307.
(23) Blessing, R. H. *Acta Crystallogr., Sect A* **1995**, *51*, 33.
(24) Sheldrick, G. M. *Acta Crystallogr., Sect. A* **1990**, *46*, 467.
(25) Sheldrick, G. M. *SHELXL-97*, Program for refinement of crystal structures; University of Göttingen, 1997.

Acknowledgment. The authors would like to thank The Royal Society for a travelling grant between the institutions and EPSRC for postdoctoral support [K.K.H.]. This work has also been supported in part by The Centre National de la Recherche Scientifique (CNRS, UMR 8640) and the Ministère de l'Education Nationale et de la Recherche et de la Technologie (Ecole Normale Supérieure).

OM9906417